An Efficient and Low-Cost Single-Stage PV Pumping System: Experimental Investigation Based on Standard Frequency Converter

Mansour MILADI*, Afef BENNANI-BENABDELGHANI**‡, Ilhem SLAMA-BELKHODJA***, Hichem M'SAAD****

* Electrical Systems Laboratory, University of Tunis El Manar, ENIT, Tunisia PHD Student, Tunis, 1002, Tunisia

** National Institute of Applied Sciences and Technologies, University of Carthage, Assistant, Tunis 1080, Tunisia.

*** Electrical Systems Laboratory, University of Tunis El Manar, ENIT, Tunisia Professor, Tunis, 1002, Tunisia

**** VOLTA PV, Tunis 1053, Tunisia

(miladi.mansour@gmail.com, afef.bennani@gmail.com, ilhem.slamabelkhodja@enit.utm.tn, hichem@voltapv.com)

‡ Corresponding Author; Mansour MILADI, University of Tunis El Manar, LSE, ENIT, BP 37 1002, Tunis le Belvedère, Tel: +216 99 890 492, miladi.mansour@gmail.com

Abstract- Economic development depends deeply on energy source availability. Solar water pumping systems are more and more important in non-electrified areas, where grid accessibility is impossible or very expensive. This paper focuses on a Solar Water Pumping System (SWPS) fed exclusively by Photovoltaic energy and using a hydraulic storage system. A finite model of the considered SWPS is given and the limitations of the scalar control for such systems are detailed. The paper proposes to add a simple and accurate control stage to the low-cost scalar control based Standard Frequency Converter (SFC) in order to improve the SWPS performances. The synthesized control is simulated and its performances are compared to conventional SFC ones: the system response time is reduced, the system shutdowns caused by a partial shadowing are minimized and the global energy intake is increased. Experimental results are shown using a laboratory test bed composed of a 2.5-kWp, 2.5-HP centrifugal pump and a 0.5-m^3 tank; and prove the effectiveness of the proposed control.

Keywords- Solar Pumping, Photovoltaic, Induction Motor, SFC, Single stage.

1. Introduction

Water and sunlight are two of the most crucial natural resources in human life. However, some environmental conditions such as the weather and the topography (deserts and mountains) have caused water supply deficiencies in many parts of the world. Hence, according to [1], [2], in 2010, one person in two had no access to potable water or to conventional sources of energy [3], [4]. In those regions, water pumping appears to be the only feasible method of ensuring water provision. The energy sources used for rural water pumping are diesel, electricity, and human or animal power. However, hand pumps are only helpful for low consumption rates and the limited availability and high cost of fuel and electricity in these areas makes their use

impracticable [5], [6]. For this reason, interest in the use of renewable energy sources has risen [7], [8]. Different electrical and hydraulic topologies are used for PV pumping systems. For the electric part, two types of motors are intensively considered: DC and asynchronous AC [9]. Various studies were initially carried out using DC motors [10], [11] since they offered a simple means of implementation with cheap power conversion [12]–[16]. Numerous operational pumping systems have shown that schemes endure from maintenance problems. To surmount this obstacle, brushless permanent magnet DC motors have been introduced [17]–[19]. Nevertheless, the power range of this application is restricted to low-power PV systems. So, more interest is directed to asynchronous machines. Induction motors based on PV pumping systems offer more

advantages in terms of reliability and maintenance because of the maturity and advances in the fields of control theory and target implementation. For these reasons, AC motors in PV systems have great impetus compared to DC ones. With consideration of the mentioned solution to this solution, two categories can be distinguished with the used power topology: motor efficiency and maximum power point tracking (MPPT) [11], [20]–[24] regarding the two-stage solution. For the second AC structure, control strategies based on open loop speed control are well adapted [25], [26]; in other works, a Standard Frequency Converter (SFC) for a variable speed drive is considered appropriate with PV pumping operation [22–24]. Recently some manufacturers have focused on dedicated PV pumping inverters based on SFC, which offers the same advantages as the converters on today's market.

A PV pumping system requires a multidisciplinary effort and its performance is strongly dependent on the system design accuracy. Authors propose an efficient methodology that, based on the geographical data of a given region, performs the design of each component of the most suitable PV pumping system [25], [30]. The first step estimates the Total Dynamic Head (TDH), the expected water flow rate, and the irradiance potential level of the studied region based on geological and metrological data provided by the corresponding and approved body of the country.

This paper focuses on investigating an open loop speed control for a Solar Water Pumping System (SWPS). In fact, we propose a modified scalar control based on DC voltage input to determine the appropriate frequency with the aim of adapting the SFC to PV pumping applications. This modified control is implemented on a low-cost numerical target and applied on an SFC. The algorithm is compared to fixed SFC frequency control and experimentally validated. The experimental results obtained reveal the innovative aspect of such an approach since it promotes electric energy intake and thus allows a better utilization of the irradiance curve. Moreover, the proposed DC voltage control demonstrates a considerable mitigation of unintentional motor-pump shutdowns.

Accordingly, we firstly describe the designed system including the PV array, the power converter, the centrifugal motor-pump, and the tank as well as the hydraulic piping. Then, the developed algorithm control is illustrated well. Simulation results are depicted and discussed in the third section. The experimental set-up is defined, the SFC architecture is explained, and the control strategy implementation is detailed. Finally, the conclusions and outlook are presented.

2. System Topology and Basic Modelling

2.1. System description

The studied SWPS system is a single power stage PV pumping installation as depicted in Fig.1. It includes three main subsystems:

- The electrical part contains the solar panels and a commercial SFC;

- The electro-mechanical part is composed of an asynchronous machine and a centrifugal pump;

- The hydraulic part contains piping equipment and one hydraulic tank.

- In this paper, the authors propose to enhance the efficiency of the considered system.
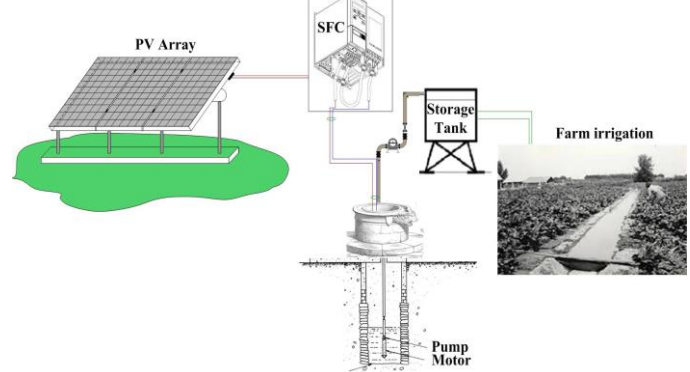
Fig. 1. PV pumping system

The SWPS sizing is based on different variables: weather conditions (the irradiance G* and the annual mean temperature T*) and geographical location, which defines the geometrical height of the well, (Hg*). Moreover a correct SPWS sizing must take into account the desired water flow, Q*, which the system will produce. These data are used to define the required technical parameters of the PV pumping system and to design its different parts by calculating [31]:

- the hydraulic motor pump rated power;

- the nominal power inverter;

- the PV array output power;

- and the tank capacity.

2.2. System modelling

To model the SPWS, the authors focus on the PV array, the SFC converter, the hydraulic part, and the induction machine. The well and the tank do not need to be dealt with.

The PV array transforms PV energy into electrical energy and the output current and voltages are governed by the I-V curve given in Fig.2.
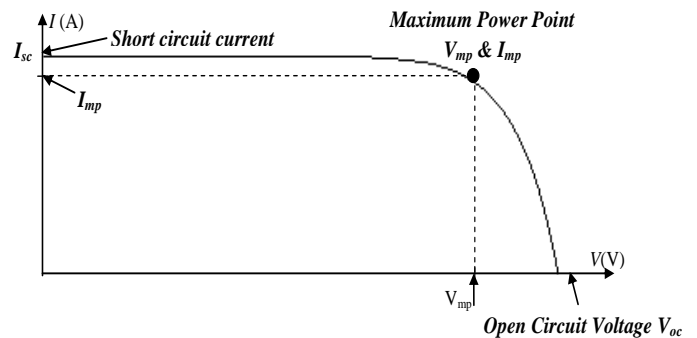
Fig. 2. PV curve characteristic in STC conditions

This characteristic can be modelled using "Eq. (1)" as described by the EN50530 standard [32], [33].

$$I_{PV} = I_{SC} - I_0 \left(e^{\frac{V_{PV}}{U_{oc}.C_{AQ}} - 1} \right) \qquad (1)$$

Where I_{sc} and U_{oc}, respectively, are the short circuit current and the open circuit voltage, which depend on the irradiance and temperature as expressed in "Eq. (2)" and "Eq. (3)":

$$I_{SC} = I_{SC,STC} \frac{G}{G_{STC}} \left(1 + \alpha(T_{PV} - T_{STC}) \right) \qquad (2)$$

$$U_{OC} = U_{OC,STC} \left(1 + \beta(T_{PV} - T_{STC}) \right) \left(\ln\left(\frac{G}{C_G} + 1 \right) C_V - C_R G \right) \qquad (3)$$

where:

G: irradiation in working conditions

G_{STC}: irradiation in the STC conditions = 1000 W/m²

T_{PV}: temperature of the PV module

T_{STC}: temperature in the STC conditions=25°C.

$I_{SC,STC}$: short-circuit current in the STC conditions

$U_{oc,STC}$: open-circuit voltage in the STC conditions

α: current temperature coefficient

β: voltage temperature coefficient

C_G, C_V, and CR: correction factors depending on panel technologies

Generally, the SFC converters contain a diode-based AC/DC bridge. For the SWPS applications, only the IGBT-based DC/AC inverter is involved to convert the DC voltage (V_{pv}) in a balanced three-phase system feeding the induction machine IM. The control algorithms of SFCs are of two types: scalar and sensorless vector control. The second one cannot be used for SPWS since it is based on the feedback control principle and the fact that the DC input voltage is constant. In this paper, only scalar control for IM is considered.

The hydraulic part (pump + piping equipment) can be modelled as an equivalent load torque as given by "Eq. (4)" [34]:

$$T_{em} = k_{pump}.\Omega^2 \qquad (4)$$

Finally, the authors focus on the IM modelling in order to define its equivalent impedance when fed by the SFC. In fact, the operating point of the SWPS, that is, the current and voltage outputs of the PV array, depend on the load equivalent impedance (SFC + induction machine + hydraulic part). Then, defining the model of this electromechanical load will allow a control that optimizes the system operation to be proposed.

The considered induction machine model is based on the steady state operation in the three-phase stationary reference frame. Fig.3 gives an equivalent one-phase model and the basic stator and rotor voltage equations are defined by "Eq. (5)".
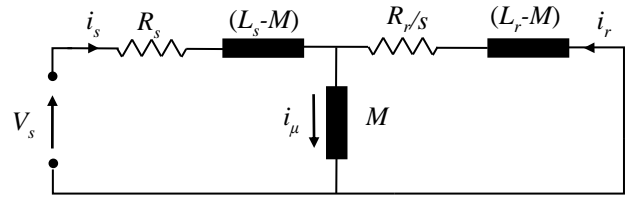
Fig. 3. Induction machine single phase equivalent circuit model

$$\begin{cases} \bar{V}_s = R_s \bar{I}_s + jL_s\omega_s\bar{I}_s + jM\omega_s\bar{I}_r \\ \bar{V}_r = 0 = R_r\bar{I}_r + jL_r\omega_r\bar{I}_r + jM\omega_r\bar{I}_s \end{cases} \qquad (5)$$

We define the equivalent impedance of the induction machine as given by "Eq. (6)". The expression of Z_m can be deduced from "Eq. (5)" and is written as "Eq. (7)" and "Eq. (8)". It is obtained from "Eq. (6)" and "Eq. (7)" as given by "Eq. (8)" and shows that the module of the machine impedance is strongly dependent on the stator pulsation, w_s, and the machine slip, s.

$$\overline{Z_m} = \frac{\bar{V}_s}{\bar{I}_s} \qquad (6)$$

$$\bar{Z}_m = R_s + j.(L_s - M) + \frac{(j.M).\left(\frac{R_r}{(s + j(L_r - M))} \right)}{\frac{R_r}{s} + j.L_r} \qquad (5)$$

$$\bar{Z}_m = R_{eq} + jX_{eq} \qquad (6)$$

where:

$R_{eq} = R_s + ((R_r/s) (M \omega_s)^2)/((R_r/s)^2 + (L_s \omega_s)^2)$ and

$X_{eq} = L_s \omega_s - ((M \omega_s)^2 L_r\omega_s)/((R_r/s)^2 + (L_r\omega_s)^2)$

To calculate the equivalent impedance Z_{SFC} of the induction machine when it is fed with the SFC, we consider the latter as a perfect Voltage Supply Inverter (VSI). Consequently, its DC input voltage V_{dc} is related to the stator machine V_{s_max} voltage according to "Eq. (10)". It can be noted that the maximum value of the stator voltage is considered in order to simplify the study and avoid dealing with the modulation index of the SFC control.

$$Z_{SFC} = \frac{V_{DC}}{I_{DC}} \qquad (9)$$

$$V_{DC} = \sqrt{3}V_{s\_max} \qquad (10)$$

Moreover, the input current of the SFC can be deduced from "Eq. (11)", where the converter losses are neglected,

leading to a perfect equality between the DC power and the active power transmitted to the induction machine.

$$I_{DC} = \frac{3.V_s.I_s.\cos\varphi_Z}{V_{DC}} \qquad (11)$$

Equations (9)–(11) yield the model of the equivalent impedance of the SFC feeding the induction machine for the studied SWPS system as given in "Eq. (12)".

$$Z_{SFC} = 2.\sqrt{R_{eq}^2 + X_{eq}^2}.\frac{1}{\cos\varphi_Z} \qquad (12)$$

Consequently, an SPWS is equivalent to a PV array feeding an electrical system where the impedance depends on the stator pulsation and the machine slip. Thus, the PV panel operation point can be controlled by means of the stator frequency reference or by adjusting the mechanical load.

In the following paragraph, a modified scalar algorithm is proposed in addition to the SFC control, in order to optimize the SPWS operation: the (I, V) operation point has to avoid the instability zone and the efficiency of the induction machine will be optimized.

3. Proposed Control

3.1. Limitation of scalar control for Solar Water Pumping Systems

The major drawbacks of the scalar-controlled SFC used for SWPSs are described below.

(i) Frequent system shutdowns: They occur mainly during cloudy days or under shaded conditions. Figs. 4.a and 4.c describe this issue: for a given system operation point at A_1, when a decrease in irradiation occurs, the new system operating point is defined by A_2. In fact, for an irradiance decrease, the (I, V) characteristic would lead to a decrease of the PV panel output voltage, V_{pv} (Fig.4.a), and an intermediate operation point A_1'. Consequently, the IM stator voltage decreases and its slip increases, as depicted in Fig. 4.b. Under these conditions, the equivalent impedance of the SWPS, described by (9), decreases as illustrated in Fig 4.c. and yields the operating point A_2, as shown in Fig 4.d.

A major decrease in V_{pv} voltage may produce a system shutdown since the SFC has a minimal input voltage value below which it stops.
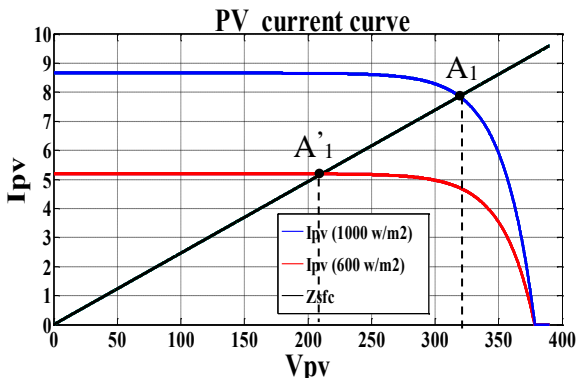
a. PV curve current for different insulations
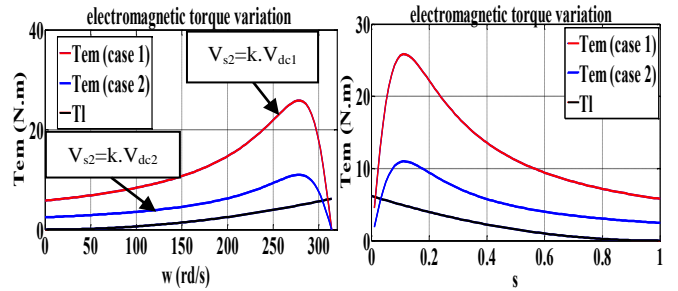
b. Electromagnetic torque variation with Vdc
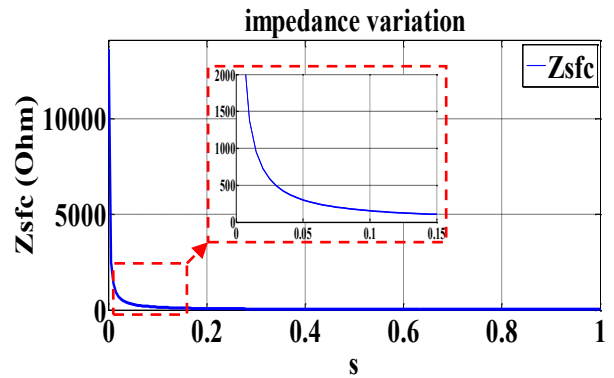
c. IM impedance change with variable irradiance
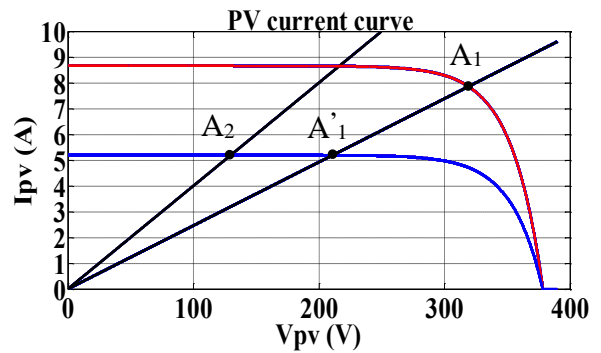
d. I-V curve operating point after shadowing
Fig. 4. Shadowing impacts on SWPS operation when fed by an SFC

(ii) As explained in part (i), the SWPS operation needs a minimal value of PV irradiation. This implies that, even for sunny periods, pumping water is possible only during limited parts of the day. Starting the system operation earlier in the morning and running it until later in the evening (i.e. with a low irradiation value) would increase the delivered power and improve the system performance.

(iii) The V/f law used in commercial SFC does not guarantee optimal machine efficiency for SWPS. This is due to the fact that the scalar control assumes that the input voltage, V_{dc}, is constant. The stator flux in the machine is then constant and its efficiency is nominal. When used with the SWPS configuration, as explained above, the input voltage V_{dc} fluctuates. It cannot be kept constant especially when meteorological conditions change. The scalar law does not guarantee a constant stator flux. On one hand, if V_{dc} decreases, the stator flux will be lower than its nominal value and the IM performances will be affected.

On the other hand, an increase in V_{dc} could lead to a hazardous flux increase and may cause damage to the machine.

It should be mentioned that the three abovementioned drawbacks are caused by the fact that the SFC operates with a constant frequency and does not take into account the specificities of PV generators. In the following paragraph, the authors propose a novel control strategy to overcome these drawbacks.

3.2. Proposed control strategy

The analysis of the drawbacks of the SWPS fed by standard SFC as described in Section 3.1 leads to the conclusion that operating at fixed frequency is the main issue for these systems. In fact, it does not allow an advantageous impedance matching of the PV generator and its load. In this paper, the authors propose a variable frequency control that would determine the frequency reference to be considered by the standard SFC in order to overcome the discussed problems. Fig. 5 gives the architecture of the proposed solution. The proposed control is a modified scalar law where the reference frequency is determined in order to adapt the IM operating point to the climatic conditions.
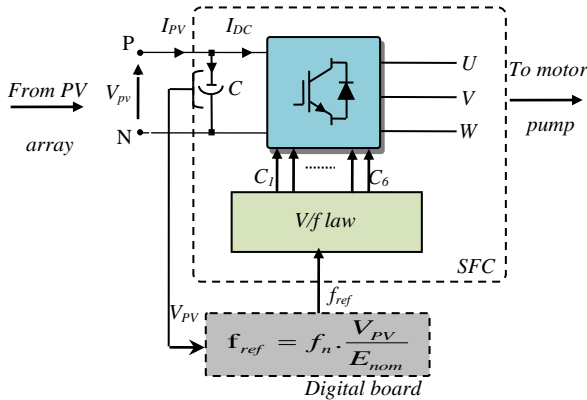
Fig. 5. Proposed SWPS structure

In order to achieve this goal, the added control step, called "frequency adaptation", calculates the reference frequency, f_{ref}, based on the measured V_{pv} voltage, as given by "Eq. (13)".

$$f_{ref} = f_n \cdot \frac{V_{PV}}{E_{nom}} \qquad (13)$$

where f_n is the stator frequency nominal value of the IM and E_{nom} is the nominal DC voltage of the SFC.

In fact, with the conventional SFC, for a chosen frequency, if the PV voltage drops due to a sudden shadow, the system could even stop since the machine impedance would decrease as explained in Section 3.1.
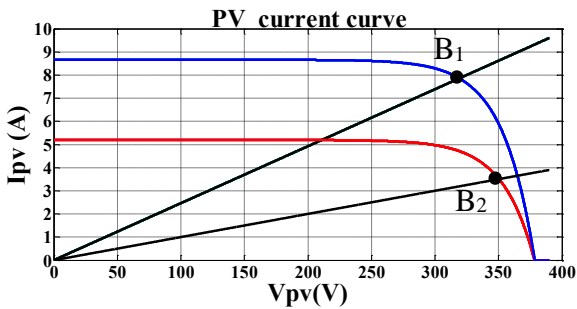
Fig. 6. Proposed control: impedance variation when Vpv change

The proposed control adapts the machine impedance to the actual PV voltage. As depicted in Fig. 6, when this voltage decreases, the reference frequency is calculated so that the machine impedance will increase, leading to a new system operating point (B_2) and avoiding the situation described in Fig.4.a.

3.3. Simulation results

Fig. 7 shows the simulated SWPS in a Matlab/Simulink environment. The PV system is composed of 14 PV panels connected in series (180 W_p), a three-phase DC/AC converter, an 1.8-kW induction machine, and a centrifugal pump modelled by $k_{pump} \cdot \Omega^2$ torque load. Firstly, the system is controlled with a conventional V/f control law and PWM strategy. Then the proposed control is introduced: the PV voltage is sensed and this measurement is used to calculate the frequency reference to be considered for the V/f control law. Furthermore, different climatic conditions are considered: the SWPS is simulated under STC conditions. Then, a low irradiance condition is investigated (G=500W/m²) to test system operation and the pumping performances around the sunrise and sunset. Finally, a sudden shadow is considered where the irradiance drops from 1000 to 500W/m².
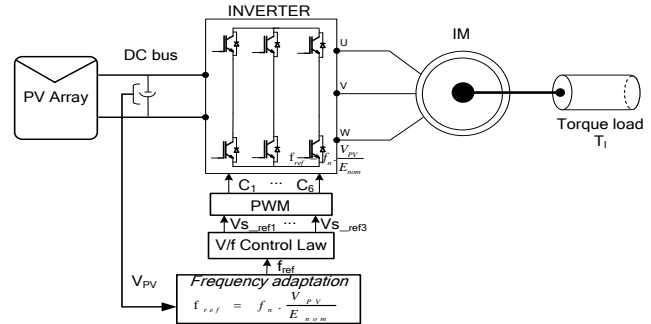
Fig. 7. Simulated solar water pumping system

a) Proposed control performance under STC conditions

Fig. 9 shows the simulation results of the SPWS performance when controlled with the proposed algorithm and with a conventional SFC one (with a reference frequency taken as 50Hz), under STC conditions (G=1000 W/m² and T=25°C). It illustrates the electric variables, PV voltage V_{pv} and PV current I_{pv} (V_s, I_s, and P_l), as well as the mechanical ones (T_l, ω). The proposed control leads to a significant improvement of the system response time. The PV panels deliver the necessary power to the pumping system after 8 seconds when a conventional SFC is used, whereas this time is reduced to 2 seconds when the proposed control is used.
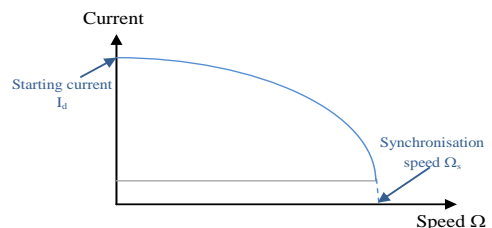
Fig. 8. Starting current value versus speed variation

As the starting current of the IM can reach a high value (Fig. 8), the resulting torque Tem will increase. However, the power generated by the PV source is limited. The V_{pv} will hence drop to 205 V and the machine needs nearly 8s to reach its steady state. This delay (i.e., 8s) can be improved by voltage control since the V/f law is adopted. So, frequency reduction allows the enhancement of the system dynamic performance. Consequently, the starting current is limited through the progressive low-voltage starting [35], [36]. Steady-state operation is similarly established for both controls. In fact, the operating point and shaft power (P_1 = 1.6-kW) remain the same.
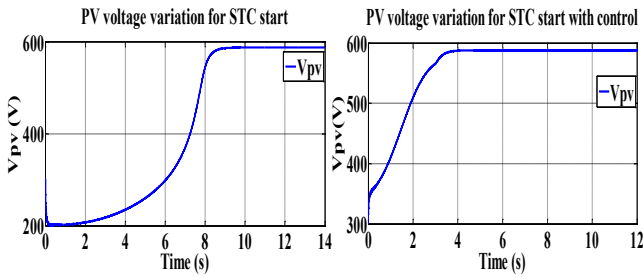
a. PV voltage variation with manual and proposed control
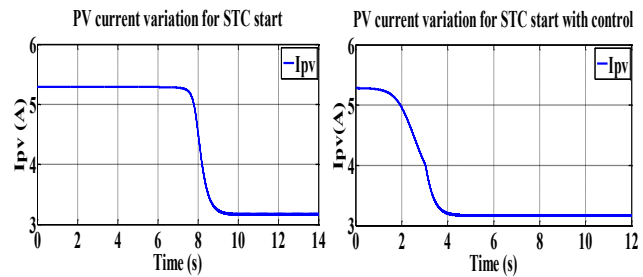
b. PV current variation with manual and proposed control
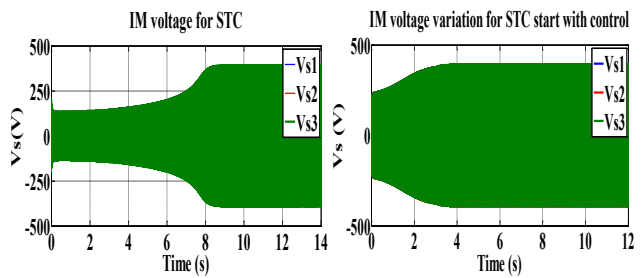
c. IM voltage variation with manual and proposed control
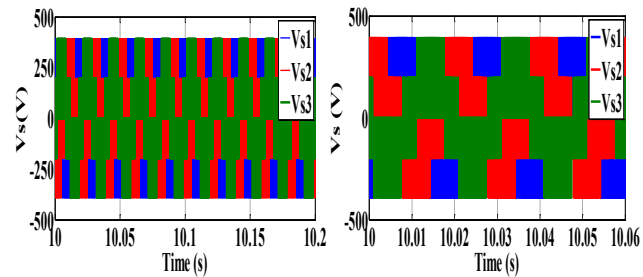
d. Magnified view of IM voltage
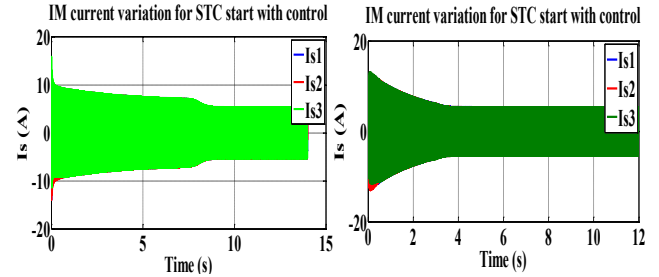
e. IM current variation
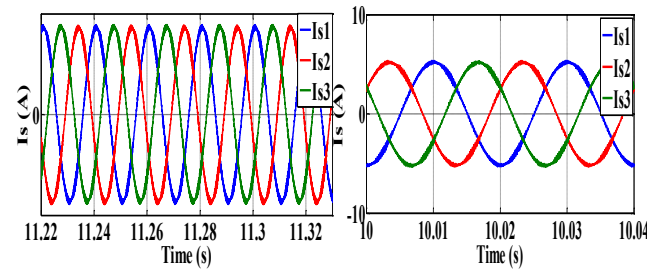
f. Magnified view of IM current
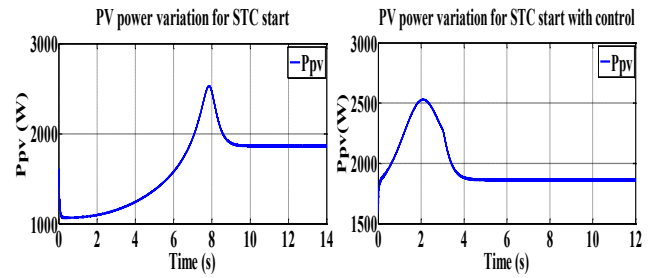
g. PV power variation with manual and proposed control
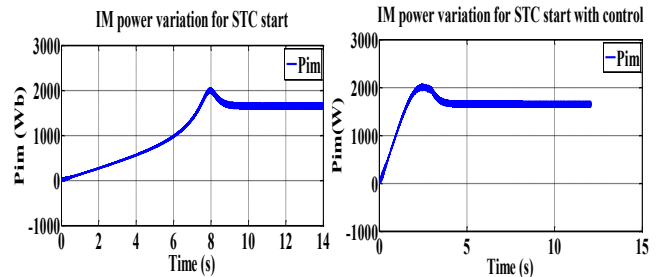
h. IM power variation with manual and proposed control
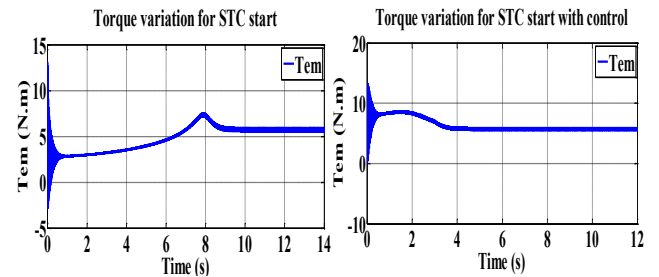
i. IM torque curves with manual and proposed control
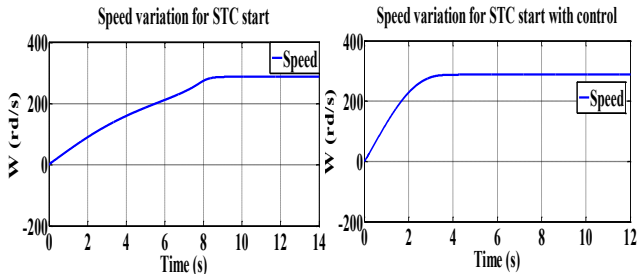
j. IM speed variation with manual and proposed control
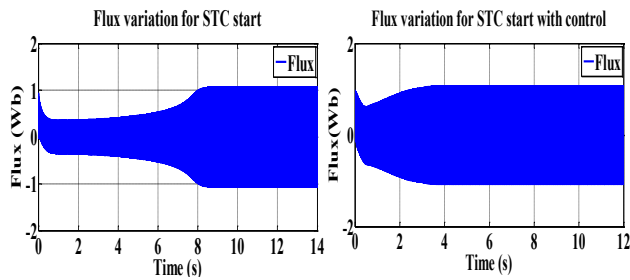
k. IM flux variation with manual and proposed control

Fig. 9. Comparison of SWPS performance between conventional and proposed control under STC conditions

b) System start with proposed control under low irradiance

The simulation results under low irradiance (G = 500W/m²; T = 25°C) are depicted in Fig. 10. In this case, the system fails to start when it is controlled with the conventional SFC control. However, with the proposed control, the system operation starts and the shaft power reach 1-kW. Thus, a better energy intake use for increasing the amount of water pumped is allowed. In fact, since the Z_{SFC} is closely linked to the reference frequency, it declines in the SFC control, leading to a V_{pv} drop and a starting system operation failure. On the other hand, the Z_{SFC} changes according to the frequency adaptation when using the proposed control and the V_{pv} does not decrease, which guarantees a better PV–load matching.
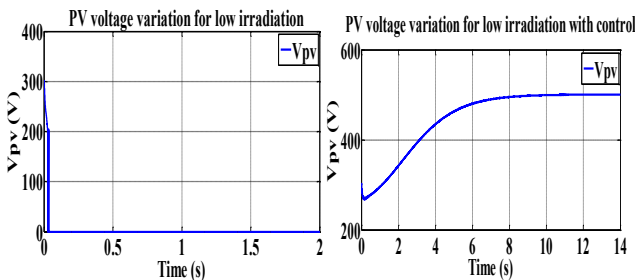
a. PV voltage variation with manual and proposed control
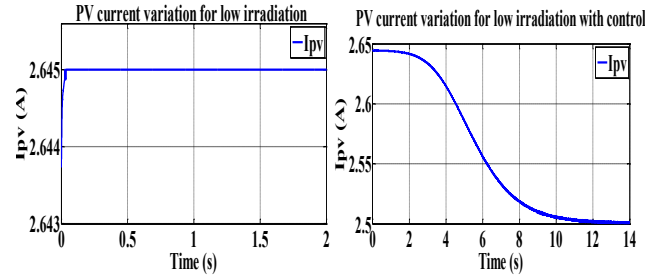
b. PV current variation with manual and proposed control
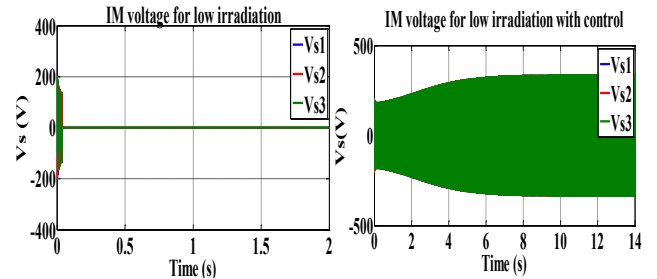
c. IM voltage variation with manual and proposed control
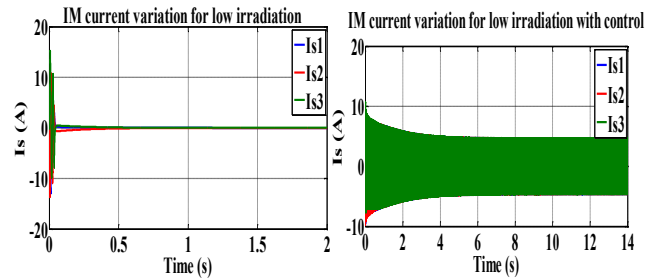
d. IM current variation
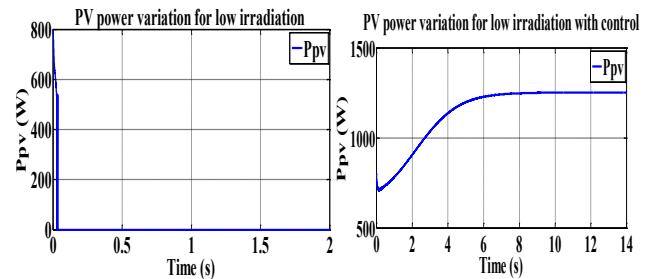
e. PV power variation with manual and proposed control
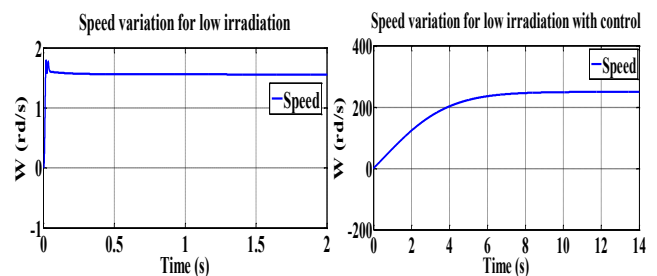
f. IM speed variation with manual and proposed control
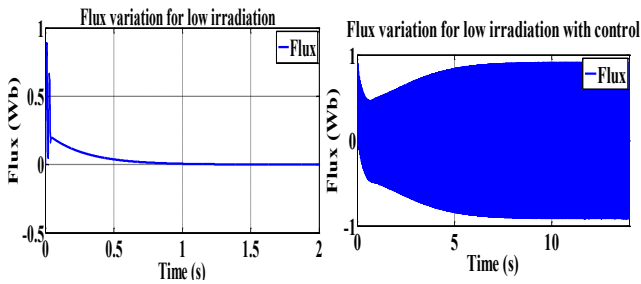
g. IM flux variation with manual and proposed control

Fig. 10. Comparison of SWPS performances between conventional and proposed control under STC conditions

c) Proposed control under partial shadowing

A comparison between the conventional and the proposed control of the system operation under partial shadowing condition is presented in Fig. 11 to validate the proper operation of the SWPS. In fact, with the conventional control, following a sudden shadowing at 9.5 s, the system converged to its steady-state operation after starting under STC conditions. When the shadowing occurred, the system decelerated until its minimal voltage value $V_{pv} = 200V$. In this operating mode, lasting 1.5 s, the system works with a reduced power and then stops. However, using the proposed control, the frequency adjustment induces Z_{SFC} variation and V_{pv} adaptation according to the change in climatic conditions. The decrease in V_{pv} is reflected in the system deceleration and consequently the torque drop. Nevertheless, the system continues to work with performances that have deteriorated but are still acceptable in steady-state operation. The flux reaches $\Phi = 0.63$ Wb and the shaft power stabilizes at 1-kW, allowing water pumping, which justifies the energy intake using the proposed control.
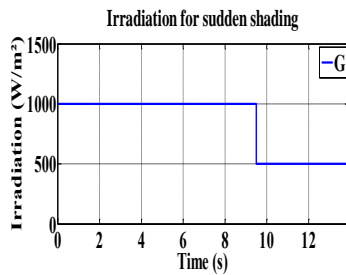
a. Irradiance variation scenario
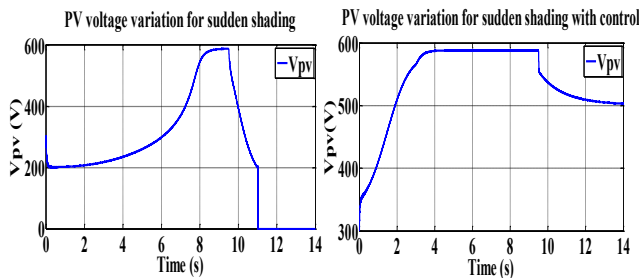
b. PV voltage variation with manual and proposed control
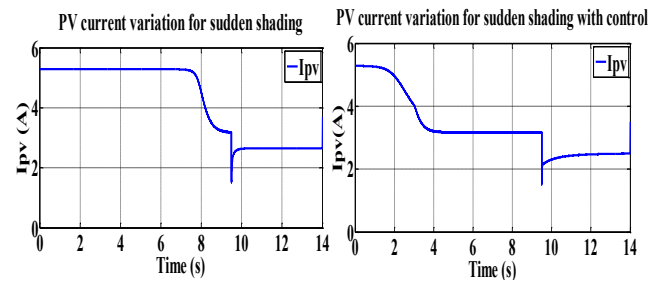
c. PV current variation with manual and proposed control
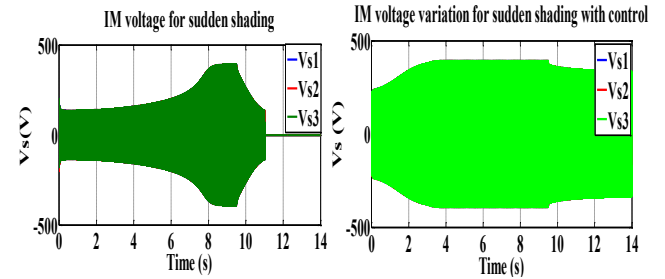
d. IM voltage variation with manual and proposed control
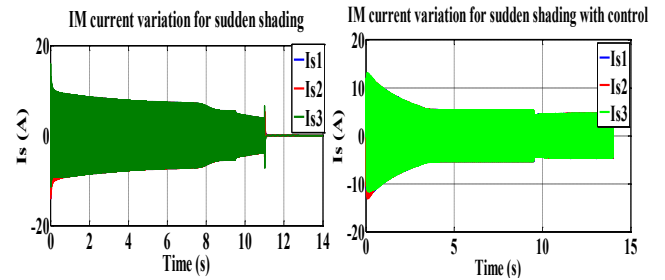
e. IM current variation
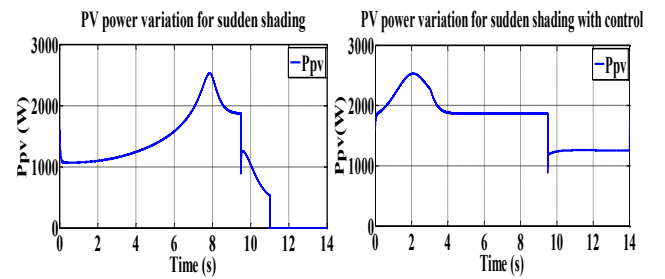
f. PV power variation with manual and proposed control
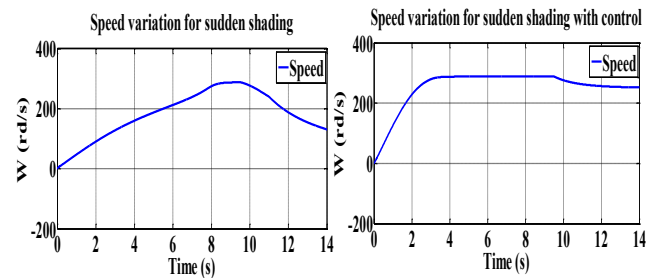
g. IM speed variation with manual and proposed control
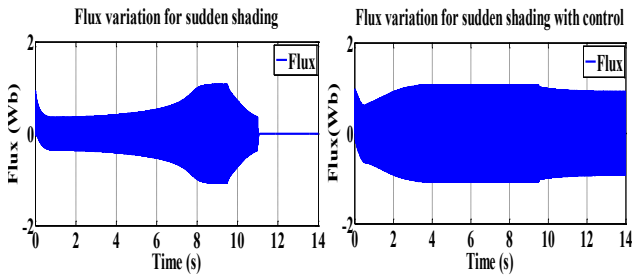
h.   IM Flux variation with manual and proposed control

Fig. 11 Comparison of SWPS performances between conventional and proposed control under sudden shading

4.   Experimental Set-up

To validate the proposed control based on the V/f law, the experimental set-up was mounted in the laboratory as shown in Fig. 12. The proposed platform contains a 2.5-kWp PV array, a 1.85-kW motor pump, one hydraulic pipe, one valve, one pressure manometer, a 0.5-m^3 tank, and an SFC, which provides the opportunity to improve the SFC performances through control algorithms implemented on a digital control board connected to the SFC.
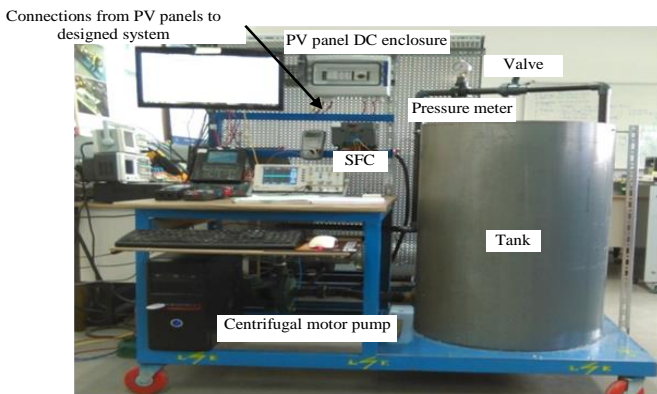
Fig. 13 shows exactly the topology of the variable speed drive on today's market, called the SFC. It is made of a rectifier bridge that converts the input from AC to DC, and an inverter that generates the variable frequency voltage from

Fig. 13. PV pumping system laboratory test bed

the DC stage. In standard operation mode, the (L, N) terminals are used as an alternative power supply.
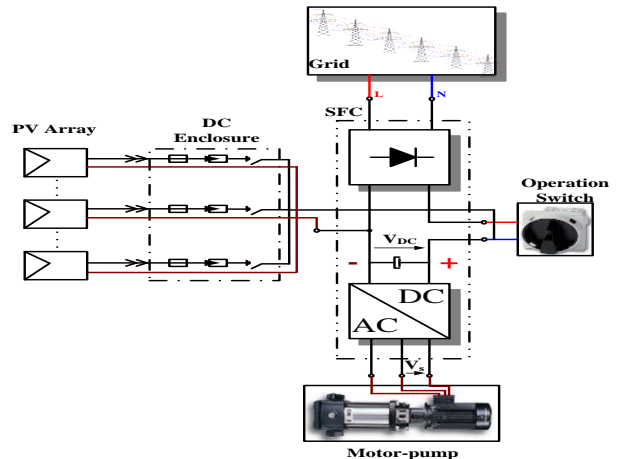
Fig. 12. Topology of the commercial SFC

Moreover, DC terminal connections (+, −) such as PV generators can be used to feed load through the inverter.

This control is achieved by the modified V/f law controller, which provides a control signal taking into account the DC voltage system evolution in order to keep it close to the reference one, which is executed indirectly by variation of the SFC operation frequency.

In commercial inverters, a DC-voltage/frequency characteristic function is normally pre-programmed within the controller unit of the inverter.

The investigated control is implemented on an STM32 microcontroller target detailed in Fig.14 and then experimentally applied on an SFC. The first step is the initialization and activation of all used peripherals (ADC, PWM, DMA, etc.) and then the main algorithm runs, waiting for interruption.

Firstly, the system operation is tested through an equivalent TDH, which gives the nominal electrical parameters at nominal speed. In fact, the valve position is fixed and kept for all the tests.

Fig. 15 shows two operation states for different frequencies.
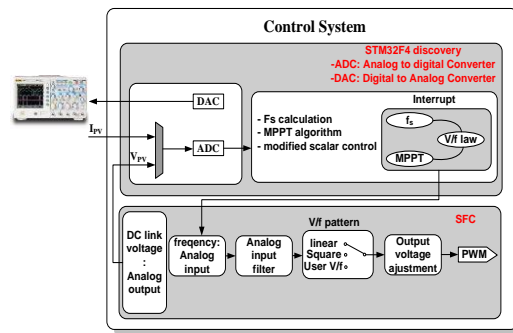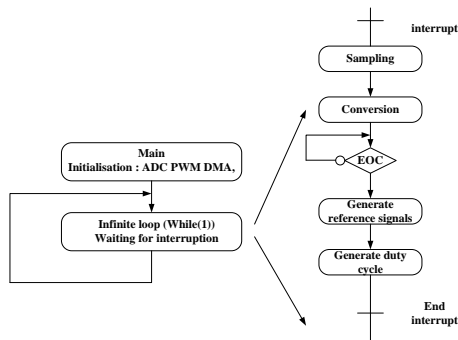
Fig. 14. System configuration and control
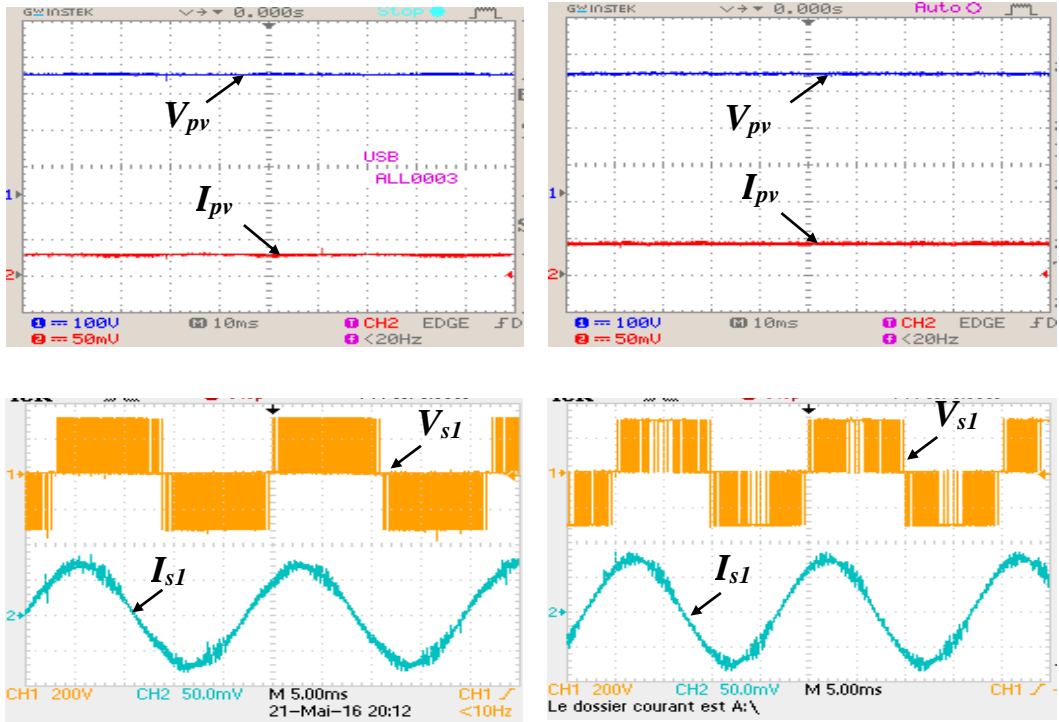
Fig. 15. Two operating points with two different frequencies
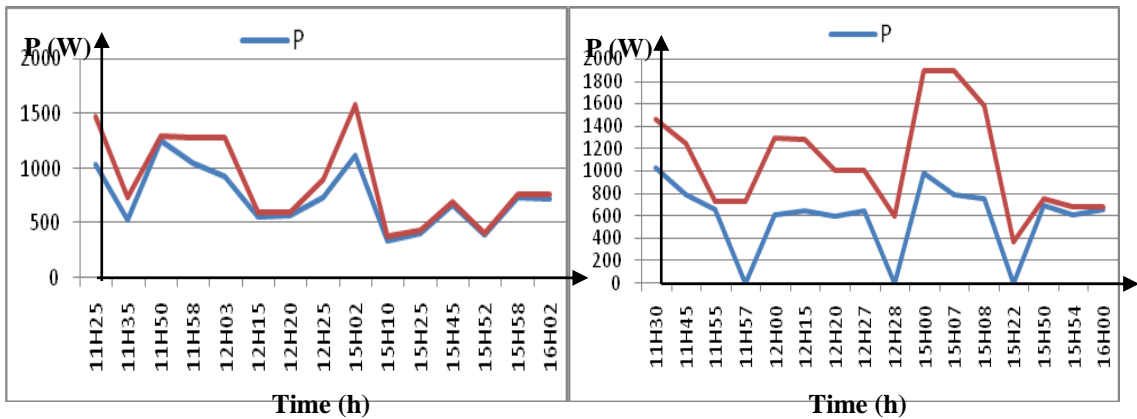
a.SWPS operation with the proposed control

b.SWPS operation with conventional SFC
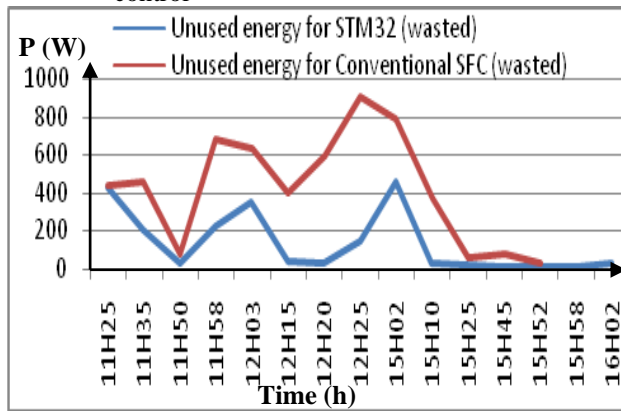
c. Energy under-exploitation for the two solutions

Fig. 16. Experimental results of the comparison of the two controls

The algorithm is compared to a fixed SFC frequency control and experimentally validated through two set of tests. The first one was realized on January, 27th, 2016 and is illustrated in Fig 16.a and the second one was realized on January, 29th, 2016 and is presented in Fig. 16.b. The first set of tests realized using an SFC fixed frequency reveals a remarkable deviation between the delivered PV power and the maximum power calculated based on real meteorological data acquired from a laboratory data logger. The second set of tests indicates the innovative aspect of the introduced approach based on dynamic frequency calculations that provide a better electric energy intake and a nominal power extraction, thus allowing a better utilization of the irradiance curve. Finally, Fig.16.c presents the under-exploitation energy for SWPS operating with conventional SFC and the proposed control. We can observe the energy intake compared with a conventional SFC. It reveals that the energy intake realized with the proposed control in one day can be double that realized by the SFC.

5. Conclusion

In this paper, we proposed a SWPS without a DC/DC stage that could be largely deployed in islanded sites thanks to its simplicity, low-cost, and reliability. First, the considered system was mathematically modelled: The PV array model is developed using the EN50530 standard, the induction machine is modeled for steady state operation and an equivalent impedance of the SFC feeding the induction machine is determined. Then, the limitations of SWPS using conventional scalar control based SFC are detailed: frequent system shutdowns, limitation of water pumping periods along the day and the fact that conventional SFC doesn't guarantee an optimal induction machine efficiency. These drawbacks were discussed and mathematically analysed thanks to the equivalent impedance model of the system described in section 2.2. The simulations result confirm the effectiveness of the synthesized modelling and the experimental results using a laboratory test bed composed of a 2.5-kWp, 2.5-HP centrifugal pump and a 0.5-m^3 tank prove the performances of the proposed control.

Acknowledgements

References

[1] P. Caton, « Design of rural photovoltaic water pumping systems and the potential of manual array tracking for a West-African village », *Sol. Energy*, vol. 103, nº Supplement C, p. 288‑302, mai 2014.

[2] "WHO | World Health Statistics 2014," WHO. [Online].Available: http://www.who.int/gho/publications/world_health_sta tistics/2014/en/. [Accessed: 14-Apr-2017].

[3] Wold Bank Group, "Addressing the Electricity Access Gap." Background Paper for the World Bank Group Energy Sector Strategy, pp. 21–29 Jun-2010..

[4] Z. Ding, M. Liu, W.-J. Lee, et D. Wetz, « An autonomous operation microgrid for rural electrification », in *2013 IEEE Industry Applications Society Annual Meeting*, 2013, p. 1‑8.

[5] A. B. Sebitosi, P. Pillay, et R. Ramakumer, « Electrification of sub-Saharan Africa », in *IEEE Power Engineering Society General Meeting, 2004.*, 2004, p. 2098‑2100 Vol.2.

[6] International Energy Agency, "World Energy Outlook 2014." pp. 5–6, 2014.

[7] S. M. Gehl, « Targets and technologies for African electrification », in *IEEE Power Engineering Society General Meeting, 2005*, 2005, p. 1828 Vol. 2-.

[8] A. Harrouz, M. Abbes, I. Colak, et K. Kayisli, « Smart grid and renewable energy in Algeria », in *2017 IEEE 6th International Conference on Renewable Energy Research and Applications (ICRERA)*, 2017, p. 1166‑1171.

[9] C. Balaji, S. S. Dash, N. Hari, et P. C. Babu, « A four port non-isolated multi input single output DC-DC converter fed induction motor », in *2017 IEEE 6th International Conference on Renewable Energy Research and Applications (ICRERA)*, 2017, p. 631‑637.

[10] S. Ryvkin et F. Himmelstoss, « Two controls of novel buck-boost converter for solar photovoltaics », in *2012 International Conference on Renewable Energy Research and Applications (ICRERA)*, 2012, p. 1‑6.

[11] M. K. Gupta, « MPPT simulation with DC submersible solar pump using output sensing direct control method and cuk converter », *Int. J. Renew. Energy Res. IJRER*, vol. 3, nº 1, p. 186–191, 2013.

[12] Z. A. Firatoglu et B. Yesilata, « New approaches on the optimization of directly coupled PV pumping systems », *Sol. Energy*, vol. 77, nº 1, p. 81‑93, 2004.

[13] H. M. B. Metwally et W. R. Anis, « Dynamic performance of directly coupled photovoltaic water pumping system using D.C. shunt motor », *Energy Convers. Manag.*, vol. 37, nº 9, p. 1407-1416, sept. 1996.

[14] M. A. Elgendy, B. Zahawi, et D. J. Atkinson, « Comparison of Directly Connected and Constant Voltage Controlled Photovoltaic Pumping Systems », *IEEE Trans. Sustain. Energy*, vol. 1, nº 3, p. 184‑192, oct. 2010.

[15] F. A. O. Aashoor et F. V. P. Robinson, « Maximum power point tracking of PV water pumping system using artificial neural based control », in *3rd Renewable Power Generation Conference (RPG 2014)*, 2014, p. 1‑6.

[16] H. P. H. Anh et N. H. Phuc, « Implementation an adaptive fuzzy NARX controller for MPPT PV supplied DC pump motor », in *2012 10th International Power Energy Conference (IPEC)*, 2012, p. 550-555.

[17] B. Singh et R. Kumar, « Solar PV array fed brushless DC motor driven water pump », in *2016 IEEE 6th International Conference on Power Systems (ICPS)*, 2016, p. 1‑5.

[18] R. Kumar et B. Singh, « Buck-boost converter fed BLDC motor drive for solar PV array based water pumping », in *2014 IEEE International Conference on Power Electronics, Drives and Energy Systems (PEDES)*, 2014, p. 1‑6.

[19] R. Kumar et B. Singh, « Solar PV array fed cuk converter-VSI controlled BLDC motor drive for water pumping », in *2014 6th IEEE Power India International Conference (PIICON)*, 2014, p. 1‑7.

[20] N. Hamrouni, M. Jraidi, A. Cherif, et A. Dhouib, « Measurements and Simulation of a PV Pumping Systems Parameters Using MPPT and PWM Control Strategies », in *MELECON 2006 - 2006 IEEE Mediterranean Electrotechnical Conference*, 2006, p. 885‑888.

[21] A. Hmidet, N. Rebei, et O. Hasnaoui, « Experimental studies and performance evaluation of MPPT control strategies for solar-powered water pumps », in *2015 Tenth International Conference on Ecological Vehicles and Renewable Energies (EVER)*, 2015, p. 1‑12.

[22] A. Betka et A. Moussi, « Performance optimization of a photovoltaic induction motor pumping system », *Renew. Energy*, vol. 29, nᵒ 14, p. 2167‑2181, nov. 2004.

[23] D. Radhakrishnan et S. S. Kumar, « Optimization of PV water pumping system with direct drive induction motor », in *2015 International Conference on Innovations in Information, Embedded and Communication Systems (ICIIECS)*, 2015, p. 1‑5.

[24] A. Belkaid, U. Colak, et K. Kayisli, « A comprehensive study of different photovoltaic peak power tracking methods », in *2017 IEEE 6th International Conference on Renewable Energy Research and Applications (ICRERA)*, 2017, p. 1073‑1079.

[25] M. Miladi, A. B. Abdelghani-Bennani, I. Slama-Belkhodja, et H. M'Saad, « Improved low cost induction motor control for stand alone solar pumping », in *2014 International Conference on Electrical Sciences and Technologies in Maghreb (CISTEM)*, 2014, p. 1‑8.

[26] A.-K. Daud et M. M. Mahmoud, « Solar powered induction motor-driven water pump operating on a desert well, simulation and field tests », *Renew. Energy*, vol. 30, nᵒ 5, p. 701‑714, avr. 2005.

[27] J. Fernández-Ramos, L. Narvarte-Fernández, et F. Poza-Saura, « Improvement of photovoltaic pumping systems based on standard frequency converters by means of programmable logic controllers », *Sol. Energy*, vol. 84, nᵒ 1, p. 101‑109, janv. 2010.

[28] M. Alonso Abella, E. Lorenzo, et F. Chenlo, « PV water pumping systems based on standard frequency converters », *Prog. Photovolt. Res. Appl.*, vol. 11, nᵒ 3, p. 179‑191, mai 2003.

[29] H. Bouzeria, C. Fetha, T. Bahi, S. Lekhchine, et L. Rachedi, « Speed Control of Photovoltaic Pumping System », *Int. J. Renew. Energy Res.*, vol. 4, nᵒ 3, p. 705–713, 2014.

[30] I. A. Odigwe, C. Nnadi, A. F. Agbetuyi, A. A. Awelewa, et F. Idachaba, « Development of a software solution for solar-PV power systems sizing and monitoring », *Int. J. Renew. Energy Res. IJRER*, vol. 3, nᵒ 3, p. 698–706, 2013.

[31] O. M. Akeyo, V. Rallabandi, et D. M. Ionel, « Multi-MW solar PV pumping system with capacity modulation and battery voltage support », in *2017 IEEE 6th International Conference on Renewable Energy Research and Applications (ICRERA)*, 2017, p. 423‑428.

[32] CENELEC, « European Standard EN 50530:Efficacité globale des onduleurs photovoltaïques raccordés au réseau ». avr-2010.

[33] S. Choudhury et P. K. Rout, « Adaptive Fuzzy Logic Based MPPT Control for PV System under Partial Shading Condition », *Int. J. Renew. Energy Res. IJRER*, vol. 5, nᵒ 4, p. 1252–1263, 2015.

[34] M. Bahloul, L. Chrifi-Alaoui, M. Souissi, M. Chabaane, et S. Drid, « Effective Fuzzy Logic Control of a Stand-alone Photovoltaic Pumping System », *Int. J. Renew. Energy Res. IJRER*, vol. 5, nᵒ 3, p. 677–685, 2015.

[35] P. L. Alger, G. Angst, et W. M. Schweder, « Saturistors and low starting current induction motors », *Electr. Eng.*, vol. 81, nᵒ 12, p. 965‑969, déc. 1962.

[36] F. D. Wijaya, S. A. Kusumawan, et H. Prabowo, « Reducing induction motor starting current using magnetic energy recovery switch (MERS) », in *2014 6th International Conference on Information Technology and Electrical Engineering (ICITEE)*, 2014, p. 1‑6.